General Relationship for the Thermal Oxidation of Silicon

B. E. DEAL AND A. S. GROVE

Fairchild Semiconductor, A Division of Fairchild Camera and Instrument Corporation,
Palo Alto, California

(Received 10 May 1965; in final form 9 September 1965)

The thermal-oxidation kinetics of silicon are examined in detail. Based on a simple model of oxidation which takes into account the reactions occurring at the two boundaries of the oxide layer as well as the diffusion process, the general relationship $x_0^2 + Ax_0 = B(t+\tau)$ is derived. This relationship is shown to be in excellent agreement with oxidation data obtained over a wide range of temperature (700°–1300°C), partial pressure (0.1–1.0 atm) and oxide thickness (300–20 000 Å) for both oxygen and water oxidants. The parameters A, B, and τ are shown to be related to the physico-chemical constants of the oxidation reaction in the predicted manner. Such detailed analysis also leads to further information regarding the nature of the transported species as well as space-charge effects on the initial phase of oxidation.

1. INTRODUCTION

OWING to its great importance in planar silicon-device technology, the formation of silicon dioxide layers by thermal oxidation of single-crystal silicon has been studied very extensively in the past several years.[1–15] Now, with the availability of large amounts of experimental data, it appears that there is much contradiction and many peculiarities in the store of knowledge of silicon oxidation. For instance, reported activation energies of rate constants vary between 27 and 100 kcal/mole for oxidation in dry oxygen; pressure dependence of rate constants has been reported as linear as well as logarithmic. While most of the data on silicon oxidation have been evaluated using the parabolic rate law, certain authors have taken recourse to using empirical power-law dependence,[14] $x_0^n = kt$, where both n and k were complex functions of temperature, pressure, and oxide thickness.

The problems associated with the latter approach can be illustrated by considering Figs 1 and 2. These figures contain a summary of data obtained in these laboratories which are in good general agreement with the corresponding data of Fuller and Strieter[14] and of Evitts, Cooper, and Flaschen.[13] (The experimental methods are dealt with in detail later.) The plots are logarithm of oxide thickness vs the logarithm of oxidation time for dry and wet oxygen (95°C H_2O) at various temperatures. The slope of the lines corresponds to the exponent n in the above power law. These values are indicated at the limiting position of some of the curves. In the case of wet oxygen (Fig. 1), n ranges from 2 for thicker oxides at 1200°C to 1 for the thinner oxide region of the 920°C data. However, for dry oxygen (Fig. 2), the value of n at 1200° approaches 2 as the oxide thickness increases above 1.0 μ; but at lower temperatures and oxide thicknesses the value of n decreases only to about 1.5 and then appears to increase again. Obviously the data cannot be represented by a simple power law.

Most of the previous theoretical treatments of the kinetics of the oxidation of metals emphasize only two limiting types of oxidation mechanisms.[16] In one, the
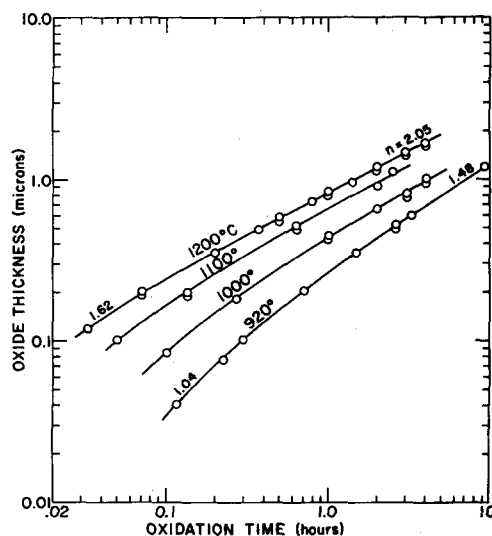
[1] J. T. Law, J. Phys. Chem. **61**, 1200 (1957).

[2] M. M. Atalla, *Properties of Elemental and Compound Semiconductors*, edited by H. Gatos (Interscience Publishers, Inc., New York, 1960), Vol. 5, pp. 163–181.

[3] J. R. Ligenza and W. G. Spitzer, J. Phys. Chem. Solids **14**, 131 (1960).

[4] J. R. Ligenza, J. Phys. Chem. **65**, 2011 (1961).

[5] W. G. Spitzer and J. R. Ligenza, J. Phys. Chem. Solids **17**, 196 (1961).

[6] M. O. Thurston, J. C. C. Tsai, and K. D. Kang, "Diffusion of Impurities into Silicon Through an Oxide Layer," Report 896-Final, Ohio State University, Research Foundation, U. S. Army Signal Supply Agency Contract DA-36-039-SC-83874, March 1961.

[7] P. S. Flint, "The Rates of Oxidation of Silicon," Paper presented at the Spring Meeting of The Electrochemical Society, Abstract No. 94, Los Angeles, 6–10 May 1962.

[8] P. J. Jorgensen, J. Chem. Phys. **37**, 874 (1962).

[9] J. R. Ligenza, J. Electrochem. Soc. **109**, 73 (1962).

[10] B. E. Deal, J. Electrochem. Soc. **110**, 527 (1963).

[11] H. Edagawa, Y. Morita, S. Maekawa, and Y. Inuishi, J. Appl. Phys. (Japan) **2**, 765 (1963).

[12] N. Karube, K. Yamamoto, and M. Kamiyama, J. Appl. Phys. (Japan) **2**, 11 (1963).

[13] H. C. Evitts, H. W. Cooper, and S. S. Flaschen, J. Electrochem. Soc. **111**, 688 (1964).

[14] C. R. Fuller and F. J. Strieter, "Silicon Oxidation," Paper presented at the Spring Meeting of The Electrochemical Society Abstract No. 74, Toronto, 3–7 May 1964.

[15] B. E. Deal and M. Sklar, J. Electrochem. Soc. **112**, 430 (1965).

[16] N. Cabrera and N. F. Mott, Rept. Progr. Phys. **12**, 163 (1948).

FIG. 1. Oxidation of silicon in wet oxygen (95°C H_2O).

oxide thickness is small in comparison to the extent of possible space-charge regions within the oxide, and the oxidation kinetics is strongly influenced by the space charge or by a voltage drop across the oxide film due to contact potential differences. In the other, the rate of diffusion of either the oxidizing species or the metal across the oxide film determines the oxidation kinetics. This latter condition leads to a parabolic relationship, $x_0 \propto t^{\frac{1}{2}}$. These two approaches have been emphasized to such an extent that deviations from parabolic oxidation have been attributed incorrectly to space-charge effects.

In this paper the oxidation kinetics are examined in greater detail. It is shown that when the reactions occurring at the two boundaries of the oxide layer are taken into account, a general relationship can be obtained with parameters which are explicitly related to the physico-chemical constants of the oxidation system. This general relationship is shown to be in excellent agreement with data obtained by various groups of investigators over a wide range of conditions. It is shown that the parameters of this relationship follow the predictions of the model. In addition, further information is obtained regarding the mechanism of oxidation: the nature of the transported species, and the role of space-charge effects.

2. GENERAL OXIDATION EQUATION

Consider silicon covered by an oxide layer of thickness x_0, as indicated in Fig. 3. In accordance with the experimental evidence for silicon, it is assumed that oxidation proceeds by the inward movement of a species of oxidant rather than by the outward movement of silicon.[2,3,8,17] The transported species must go through the following stages:

(1) It is transported from the bulk of the oxidizing gas to the outer surface where it reacts or is adsorbed.

(2) It is transported across the oxide film towards the silicon.

(3) It reacts at the silicon surface to form a new layer of SiO_2.

It is assumed in this paper that the oxidation process is beyond an initial transient period with the consequence that the fluxes of oxidant in each of the above three steps are, at all times, identical. (The flux of oxidant is the number of oxidant molecules crossing a unit surface area in a unit time.) The validity of this steady-state assumption is shown in the Appendix. The steady-state fluxes are approximated as follows.

The flux of the oxidant from the gas to the vicinity of the outer surface is taken to be

$$F_1 = h(C^* - C_0), \qquad (1)$$

[17] W. A. Pliskin and R. P. Gnall, J. Electrochem. Soc. 111, 872 (1964).
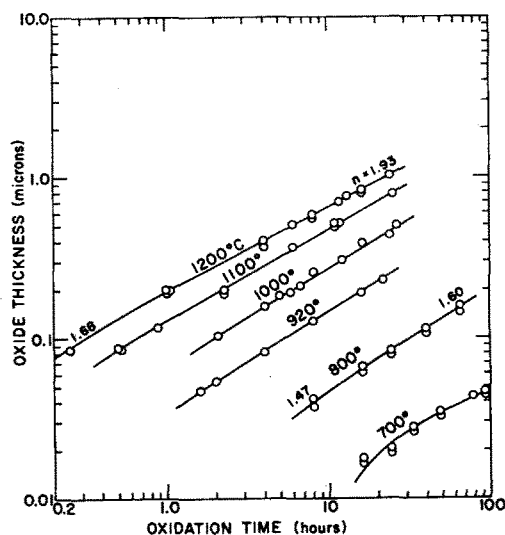
Fig. 2. Oxidation of silicon in dry oxygen (760 Torr).

where h is a gas-phase transport coefficient, C_0 is the concentration of the oxidant at the outer surface of the oxide at any given time, and C^* is the equilibrium concentration of the oxidant in the oxide. (This linearized approximation to the transport rate is analogous to Newton's law of cooling.) Note that when $C_0 = C^*$, $F_1 = 0$. The equilibrium concentration of the oxidant is assumed to be related to the partial pressure of the oxidant in the gas by Henry's law,

$$C^* = Kp. \qquad (2)$$

Henry's law only holds in the absence of dissociation or association of the oxidant at the outer surface. Thus, the oxidant is assumed to be molecular O_2, and H_2O in the cases of dry- and wet-oxygen oxidation, respectively. The experimental evidence will be seen to justify this assumption.
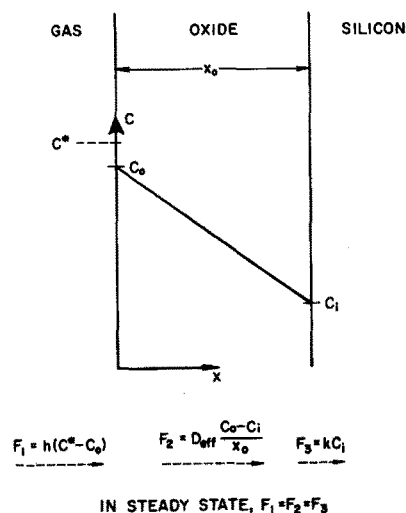
Fig. 3. Model for the oxidation of silicon.

The flux of the oxidant across the oxide layer is assumed to be given by Fick's law,

$$F_2 = -D_{eff}(dC/dx), \tag{3}$$

at any point x within the oxide layer, where D_{eff} is the effective diffusion coefficient and dC/dx is the concentration gradient of the oxidizing species in the oxide.

It follows from the assumption of steady-state oxidation that F_2 must be the same at any point x within the oxide film, or that $dF_2/dX = 0$. Consequently, the concentration of the oxidant within the oxide layer is linear as indicated in Fig. 3, and the flux F_2 is given by

$$F_2 = D_{eff}(C_0 - C_i)/x_0, \tag{4}$$

where C_i is the concentration of the oxidant near the oxide–silicon interface.

If the transported species are ionic, they set up a space charge within the oxide film. The effective diffusion coefficient D_{eff} incorporates the effect of such space charges in enhancing the rate of transport. It was shown by Cabrera and Mott,[16] as well as by Bardeen, Brattain, and Shockley,[18] that if the oxide thickness is large enough in comparison to the thickness of the space-charge regions, D_{eff} is approximately twice the actual diffusion coefficient. The extent of the space-charge region in SiO$_2$ films is shown later to be of the order of 200 Å, or less, so that this condition is met in most practical cases.

Finally, the flux corresponding to the oxidation reaction is expressed by the first-order relation

$$F_3 = kC_i. \tag{5}$$

Noting that $F_1 = F_2$ and $F_2 = F_3$ due to the steady-state condition, and solving for C_i and C_0 between these two equations, one obtains

$$\frac{C_i}{C^*} = \frac{1}{1 + k/h + kx_0/D_{eff}}, \tag{6}$$

and

$$\frac{C_0}{C^*} = \frac{1 + kx_0/D_{eff}}{1 + k/h + kx_0/D_{eff}}. \tag{7}$$

Note that in the limit where the diffusivity becomes very small relative to the rate constants associated with surfaces, k and h (i.e., $D_{eff}/kx_0 \to 0$), $C_i \to 0$ and $C_0 \to C^*$. This condition is commonly referred to as "diffusion controlled."

With C_i and C_0 eliminated, the flux is given by

$$F = F_1 = F_2 = F_3 = \frac{kC^*}{1 + k/h + kx_0/D_{eff}}. \tag{8}$$

If N_1 is the number of oxidant molecules incorporated into a unit volume of the oxide layer, the rate of growth

of the oxide layer is described by the differential equation

$$\frac{dx_0}{dt} = \frac{F}{N_1} = \frac{kC^*/N_1}{1 + k/h + kx_0/D_{eff}}. \tag{9}$$

To arrive at a general initial condition to this equation, the total oxide thickness x_0 is taken to consist of two parts: an initial layer of oxide x_i that might have been present on the silicon prior to the oxidation step under consideration, and the additional thickness grown during the step under consideration. Thus the initial condition for this step is:

$$x_0 = x_i \quad \text{at} \quad t = 0. \tag{10}$$

Such division of the oxide layer is not only important because it permits consideration of multiple oxidations, but also because x_i can be regarded as the thickness of the layer grown before the approximations of the above treatment become valid. Thus, an initial oxide layer may be formed by mechanisms involving fields and space charges within the oxide layer.[16]

The solution of the differential equation, Eq. (9), subject to the initial condition, Eq. (10), obtained by a straightforward integration, is

$$x_0^2 + Ax_0 = Bt + x_i^2 + Ax_i, \tag{11}$$

which can be rewritten in the form

$$x_0^2 + Ax_0 = B(t + \tau), \tag{12}$$

where

$$A \equiv 2D_{eff}(1/k + 1/h), \tag{12a}$$

$$B \equiv 2D_{eff}C^*/N_1, \tag{12b}$$

and

$$\tau \equiv (x_i^2 + Ax_i)/B. \tag{12c}$$

The quantity τ corresponds to a shift in the time coordinate which corrects for the presence of the initial oxide layer x_i. The form of this mixed parabolic relationship was first proposed by Evans.[19,20]

Solving the quadratic equation (12) yields the form

$$\frac{x_0}{A/2} = \left[1 + \frac{t + \tau}{A^2/4B}\right]^{\frac{1}{2}} - 1, \tag{13}$$

which gives the oxide thickness as a function of time.

It is interesting to examine two limiting forms of Eq. (13). At relatively large times, i.e., $t \gg A^2/4B$, and also $t \gg \tau$,

$$\frac{x_0}{A/2} \cong \left(\frac{t}{A^2/4B}\right)^{\frac{1}{2}}$$

or

$$x_0^2 \cong Bt. \tag{14}$$

Thus, the general relation, Eq. (13), reduces to the well-known parabolic oxidation law for relatively long

[18] J. Bardeen, W. H. Brattain, and W. Shockley, J. Chem. Phys. 14, 714 (1946).

[19] U. R. Evans, Trans. Electrochem. Soc. 46, 247 (1924).
[20] U. R. Evans, *The Corrosion and Oxidation of Metals* (Edward Arnold and Company, London, 1960), pp. 819–859.

times. The coefficient B, as given by Eq. (12b), is identical with that derived by Cabrera and Mott.[16] It is referred to as the *parabolic rate constant*.

At the other extreme, for relatively small oxidation times, i.e., $t \ll A^2/4B$,

$$\frac{x_0}{A/2} \cong \frac{1}{2}\left(\frac{t+\tau}{A^2/4B}\right)$$

or

$$x_0 \cong \frac{B}{A}(t+\tau). \tag{15}$$

Thus, the general relationship reduces to a linear law. The coefficient

$$\frac{B}{A} = \frac{kh}{k+h}\left(\frac{C^*}{N_1}\right)$$

is referred to as the *linear rate constant*. The general relationship and its two limiting forms are shown in Fig. 12, together with experimental points which are discussed later. It should be noted at this point, however, that for most of the range the parabolic limit does not provide a good approximation. For this reason, simply dividing x_0^2 by t does not necessarily yield the true parabolic rate constant B, but rather it gives some quantity which may or may not approximate B depending on the oxidation conditions and the time. Thus, it appears that many of the contradictions referred to in the Introduction may well have been due to forcing the parabolic law in regions where it could not provide a meaningful fit.

3. EXPERIMENTAL METHODS

The oxidation apparatus used in this program was similar to that used in previous investigations.[10,15] Either purified dry oxygen (water content less than 5 ppm) or wet oxygen (oxygen bubbled through water at 95°C) could be supplied to the quartz oxidation tube. The partial pressure of water in the wet-oxygen ambient was estimated to be 640 Torr. Silicon slices were placed flat on a quartz boat during oxidation. Oxidation temperature was controlled to ± 1°C over the range 700° to 1200°C.

Silicon used was in the form of circular slices 22 mm in diameter and mechanically polished to 200 μ thickness. It was (111) surface oriented, Czochralski pulled, with an initial dislocation count of less than 100 cm^{-2}. Silicon resistivity was 1.3 $\Omega \cdot$cm, p-type boron doped ($C_B = 1.45 \times 10^{16}$ cm^{-3}). Cleaning procedures prior to oxidation included both organic and inorganic rinses using ultrasonic agitation to insure noncontaminated surfaces.

Oxide thicknesses were determined using multiple-beam interferometric techniques. Accuracy of the measurement for oxides thicker than 0.20 μ was ± 40 Å. For thinner oxides, the accuracy was ± 25 Å.
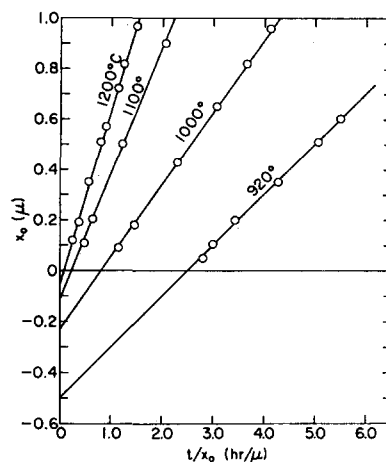
FIG. 4. Evaluation of rate constants for oxidation of silicon in wet oxygen (95°C H_2O). Slopes of lines correspond to B in Eq. (12), intercepts at $t/x_0 = 0$ correspond to $-A$ in Eq. (12).

4. EXPERIMENTAL RESULTS

A. Wet Oxygen

To check how well the general oxidation equation, Eq. (12), fits the data, the following procedure was employed.[20] First, a detailed plot of oxide thickness vs oxidation time was made to determine what initial oxide thickness x_i the data extrapolated to at $t=0$. In the case of wet-oxygen oxidation x_i was found to be zero at all temperatures. Then the oxide thickness x_0 was plotted vs the quantity t/x_0. As can be seen from Eq. (12), if that relationship holds and $\tau = 0$, such a plot should yield straight lines with intercept equal to $-A$, and slope equal to B.

Wet oxygen data from Fig. 1 are plotted in this manner in Fig. 4. Straight lines are indeed obtained for all four temperatures with the absolute values of A increasing with decreasing temperatures. At the same time, values of the slope B decrease with decreasing temperature. Values of the constants A and B determined from this plot for the four temperatures are tabulated in Table I. Analysis of the data has indicated that the precision of the constant B is $\pm 2\%$ over the entire range of measurements. For larger values of A (low temperatures) the precision is $\pm 2\%$. In the case of high temperatures, the precision of A is $\pm 12\%$. It should be noted that this larger deviation at higher temperatures is not especially critical, since A itself

TABLE I. Rate constants for oxidation of silicon in wet oxygen (95°C H_2O). $x_0^2 + Ax_0 = B(t+\tau)$.

Oxidation temperature (°C)	A (μ)	B (μ^2/h)	B/A (μ/h)	τ(h)
1200°	0.05	0.720	14.40	0
1100°	0.11	0.510	4.64	0
1000°	0.226	0.287	1.27	0
920°	0.50	0.203	0.406	0
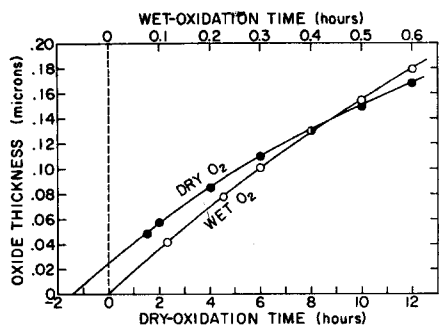
FIG. 5. Comparison of initial oxide growth at 920°C for oxidation in wet-(95°C H_2O) and dry-oxygen ambients.

is very small and hence its influence on the oxidation rate becomes less important.

Special experiments demonstrated that the values of A and B are essentially the same when the carrier-gas oxygen is replaced by argon. Thus, the effect of the oxygen in the wet-oxygen atmosphere can be neglected under the conditions of these experiments, with the implication that the oxidizing species is water.

B. Dry Oxygen

In contrast to the case with wet oxygen, a detailed plot of oxide thickness vs time for dry oxygen did not extrapolate to zero initial thickness at any of the experimental temperatures. The difference between the wet- and dry-oxygen cases is illustrated in Fig. 5. Here both dry- and wet-oxygen data at 920°C are plotted in the same graph with the time scales adjusted to provide similar curve ` shapes. While the wet-oxygen data extrapolate to zero, the plot for dry oxygen appears to pass through the thickness axis at $x_0 = 250$ Å. This was found to be the case for all temperatures from 700° to 1200°C, with the intercept being in all cases 230 ± 30 Å. A re-examination of Fig. 2 shows that the differences in the variation of the exponent n in the empirical power-law formula, $x_0{}^n = kt$, between wet- and dry-oxygen oxidation described in the Introduction are in fact due to this phenomenon. Consideration of the corresponding data of Fuller and Strieter[14] and of Evitts
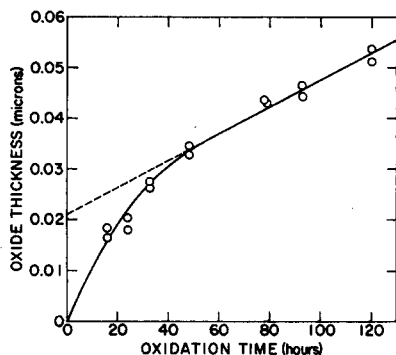
FIG. 6. Oxidation of silicon in dry oxygen at 700°C.

et al.[13] lead to the same conclusion: an offset of about 200 Å in the thickness data when extrapolated to $t = 0$.

This finding could mean one of two things. Either an oxide film of this order of thickness was originally present before the oxidations were started, or a different mechanism of oxidation prevailed at oxide thicknesses less than 300 Å. The latter was assumed to be the case, since no initial oxide could be detected by experimental techniques. In addition, the wet-oxygen data indicated no initial oxide and the silicon preparation was identical for the two types of oxidation. Further confirmation was provided by precise and detailed measurements at 700°C. A plot of oxide thickness vs time at 700°C is shown in Fig. 6. It can be observed that an initial rapid rate of oxidation occurs, followed by a strictly linear process which extrapolates back to $x_0 = 210$ Å at $t = 0$.

Thus, for oxidation in dry oxygen, the initial condition $x_i = 230$ Å was adopted. The corresponding values of $\tau \equiv (x_i{}^2 + Ax_i)/B$ were estimated graphically by plotting x_0 vs t and extrapolating the curve back through
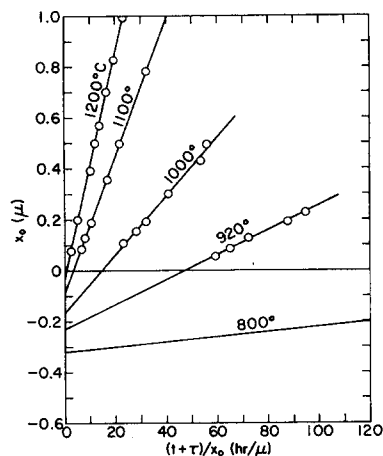
FIG. 7. Evaluation of rate constants for oxidation of silicon in dry oxygen. Slopes of lines correspond to B in Eq. (12), intercepts at $(t+\tau)/x_0 = 0$ correspond to $-A$ in Eq. (12).

$x_i = 230$ Å to the time axis. The value of τ varies with temperature even though x_i is a constant since A and B are a function of temperature.

In Fig. 7, x_0 is plotted vs $(t+\tau)/x_0$. (Values of $(t+\tau)/x_0$ for 800°C are of the order of 400 h/μ. For this reason, only the line extrapolated from these data is shown in Fig. 7.) The resulting rate constants for dry oxygen are given in Table II. In the case of 700°, the relationship was found to be completely linear and therefore only the ratio B/A could be determined. The precision of these constants is of the same order as discussed for the wet-oxidation results. The significance of the finite x_i is discussed later.

C. Pressure Dependence of Rate Constants

According to Eq. (12), the parabolic rate constant B should be proportional to C^*, which in turn should be

TABLE II. Rate constants for oxidation of silicon in dry oxygen. $x_0^2 + A x_0 = B(t+\tau)$.

Oxidation temperature (°C)	A (μ)	B (μ^2/h)	B/A (μ/h)	τ (h)
1200°	0.040	0.045	1.12	0.027
1100°	0.090	0.027	0.30	0.076
1000°	0.165	0.0117	0.071	0.37
920°	0.235	0.0049	0.0208	1.40
800°	0.370	0.0011	0.0030	9.0
700°	⋯	⋯	0.00026	81.0

proportional to the partial pressure of the oxidizing species in the gas if Henry's law is obeyed. Conversely, the coefficient A should be independent of the partial pressure. Data presented by Flint[7] on oxidation of silicon with various partial pressures of oxygen or water vapor in argon were examined. It was found through plots of x_0 vs $(t+\tau)/x_0$ that A was a constant over a range of partial pressures, while the value of B was directly proportional to the partial pressure, at all experimental temperatures. This dependence is illustrated in Fig. 8. Here the values of B, normalized to the 760-Torr value at each temperature are shown as a function of the partial pressure of the oxidizing species—O_2 or H_2O, respectively—in the gaseous ambient. (The 760-Torr value was determined by correcting the wet-O_2 data of the present investigation from 640 to 760 Torr using the linear relationship. Values obtained by this extrapolation closely agreed with Flint's[7] data based on oxidation in atmospheric steam.) A very good linear dependence is observed for temperatures ranging between 1000° and 1200°C.

D. Temperature Dependence of Rate Constants

In Fig. 9, the logarithm of the parabolic rate constant B is plotted against the reciprocal of the absolute temperature for both dry- and wet-oxygen oxidation. Also shown are the wet-oxygen values correlated to 760-Torr water vapor pressure using the linear pressure dependence. As is evident, good straight lines are obtained in all cases.

According to Eq. (12b), the temperature dependence of B should be substantially the same as that of D_{eff}. For dry oxygen, the activation energy of B is found to be 28.5 kcal/mole from Fig. 9. This can be compared to the value of 27.0 kcal/mole reported by Norton[21] for the diffusivity of oxygen through fused silica. (The structure of the SiO_2 formed by thermal oxidation of silicon corresponds to that of amorphous, fused silica.) The activation energy for wet-oxygen oxidation is 16.3 kcal/mole, in reasonably good agreement with the 18.3-kcal/mole value found by Moulson and Roberts[22] for the diffusivity of water in fused silica. These diffusivity values are shown in Fig. 10 for reference.

[21] F. J. Norton, Nature 171, 701 (1961).
[22] A. J. Moulson and J. P. Roberts, Trans. Faraday Soc. 57, 1208 (1961).
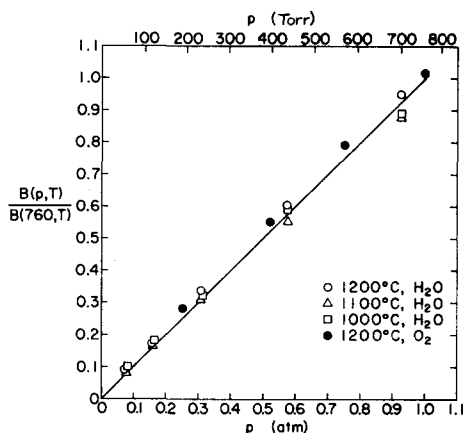
FIG. 8. The effect of partial pressure of the oxidant on the parabolic rate constant. Rate constants are normalized to the 760-Torr value at the same temperature. (Flint's[7] data for wet and dry oxygen, 1000° to 1200°C).

The temperature dependence of the linear rate constant B/A is shown in Fig. 11. Exponential temperature dependence is obtained again for both the dry- and wet-oxygen cases. The activation energies 46.0 and 45.3 kcal/mole for dry- and wet-oxygen oxidation, respectively, are almost identical, indicating a similar surface-control mechanism for the two oxidants.

E. Equilibrium Solubility Concentrations

The equilibrium concentration C^* of the oxidants oxygen and water in SiO_2 can be calculated using Eq. (12b). Parabolic rate constants are taken from Fig. 9, diffusivities from Fig. 10, N_1 for oxygen is 2.25×10^{22} cm^{-3}, while the corresponding value for
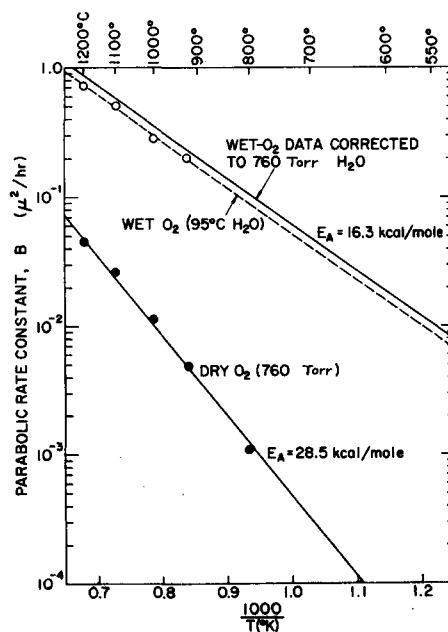
FIG. 9. The effect of temperature on the parabolic rate constant B,

water is twice this number. The resulting values of C^* at 1000°C are listed in Table III.

Also shown in Table III are the equilibrium solubilities of these two species in fused silica as determined by Norton[21] through permeation experiments and by Moulson and Roberts[22] through infrared-absorption experiments, respectively. The agreement between these values and the C^* results obtained from the oxidation data is indeed excellent. Since the temperature dependence of B and of D_{eff} were found to be substantially the same, similar values of C^* would be obtained at any other temperature within the experimental range. Such a conclusion is substantiated by Moulson and Roberts, who found an essentially constant solubility of water in fused silica between 900° and 1200°C.

F. Surface-Reaction Rate Constants

The linear rate constants determined in Sec. 4(A) and (B),

$$\frac{B}{A} = \frac{kh}{k+h}\left(\frac{C^*}{N_1}\right),$$

contain the effects of the phenomena taking place both at the gas–oxide interface, through h, and at the oxide–silicon interface, through k. If these two constants are very different in magnitude, the quantity $kh/(k+h)$ will approximately equal k or h, whichever is smaller.

This quantity can be calculated from the experimentally measured linear rate constants B/A, the known values of N_1, and the values of the equilibrium solubility concentrations C^*, as determined in the previous section. Thus, the value of $kh/(k+h)$ is calculated to be 3.6×10^4 μ/h for dry O_2 and 1.8×10^3 μ/h for wet O_2, at 1000°C. If it is now assumed that h is determined solely by a gas-phase transport process, its value can be estimated on the basis of standard boundary-layer considerations[23] to be about 10^8 μ/h for the present flow conditions (Reynolds number ≈ 25). Since this is several orders of magnitude larger than the above values of $kh/(k+h)$, it follows that

$$\frac{kh}{k+h} \doteq k = \begin{cases} 3.6\times10^4 \ \mu/h \text{ for dry-}O_2 \\ 1.8\times10^3 \ \mu/h \text{ for wet-}O_2 \end{cases} \text{ oxidation}$$

at 1000°C. Thus, the activation energies reported in Sec. 4D, 46.0 and 45.3 kcal/mole, respectively, reflect the temperature dependence of the interfacial reaction-rate constant k. These values may be compared with 42.2 kcal/mole, the energy required to break an Si–Si bond (as given by Pauling,[24] p. 85).

[23] H. Schlichting, *Boundary Layer Theory* (McGraw-Hill Book Company, Inc., New York, 1960), 4th ed., Chap. 14; and R. B. Bird, W. E. Stewart, and E. N. Lightfoot, *Transport Phenomena* (John Wiley & Sons, Inc., New York, 1960), Paragraph 21.2.
[24] L. Pauling, *The Nature of the Chemical Bond* (Cornell University Press, Ithaca, New York, 1960), 3rd ed.
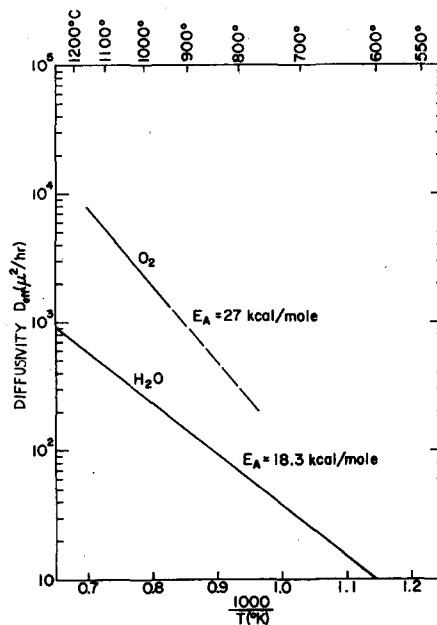
FIG. 10. The diffusivity of oxygen (Norton[21]) and of water (Moulson and Roberts[22]) in fused silica as a function of temperature.

The relatively large value of the gas-phase transport coefficient h is confirmed by two other experiments. In one, the carrier-gas flow rate was varied 50-fold without any significant effect on the oxidation rate. In the other, it has been noted[10] that the backside of a slice lying flat on the boat was oxidized to the same extent as its topside. Both of these observations point to the relatively small importance of the gas-phase transport process in controlling the over-all oxidation rate.

5. DISCUSSION

In summary a simple model of the oxidation process has been developed, and then compared to experimental results obtained over a wide range of variation of conditions: ambient pressure and temperature. It was found that the general relationship, Eq. (12), is obeyed by silicon oxidation throughout this range. Furthermore, the coefficients of this relationship were shown to depend in the predicted manner on pressure and temperature. Thus, the parabolic rate constant B is proportional to the partial pressure of the oxidant in the gas (O_2 and H_2O, respectively) while the coefficient A is independent

TABLE III. Solubility of oxidizing species in SiO_2 at 1000°C.

Species	Solubility (cm^{-3})	
	This work (C^*)	Other methods
O_2	5.2×10^{16}	5.5×10^{16} (permeation)[21]
H_2O	3.0×10^{19}	3.4×10^{19} (infrared)[22]

of the pressure. The temperature dependence of the parabolic rate constant is exponential, with the activation energies corresponding to the available activation energies for the diffusivities of oxygen and of water through fused silica. Finally, the equilibrium solubility concentrations C^* determined from the rate constants are in good agreement with the solubility of oxygen and water in fused silica as determined by other methods. This general agreement serves as an indication of the validity of the assumptions made in the derivation of Eq. (12).

The general relationship for the oxidation of silicon is illustrated in Fig. 12. Large numbers of oxidation data, including results shown in Figs. 1 and 2, earlier measurements obtained at these laboratories,[7] and the work of two other groups of investigators,[13,14] were reduced using the parabolic and linear rate constants given in Figs. 9 and 11 and the pressure dependence shown in Fig. 8. Then, these data were plotted following the rearranged form of the general oxidation relationship, Eq. (13). Included as a solid line (almost masked out by the experimental data) is a calculated plot corresponding to the general relationship $x_0^2 + Ax_0 = B(t+\tau)$. The excellent over-all agreement is quite evident and speaks for the validity and usefulness of the general relationship.

Figure 12 also shows the two asymptotic forms of the general relationship: the parabolic law valid at "large" times and the linear law valid at "small" times. It is important to note that the criterion of "small" or "large" times depends on the oxidation conditions, as reflected in the Parameters A and B. Thus, this criterion is that the time should be smaller (or larger) than the
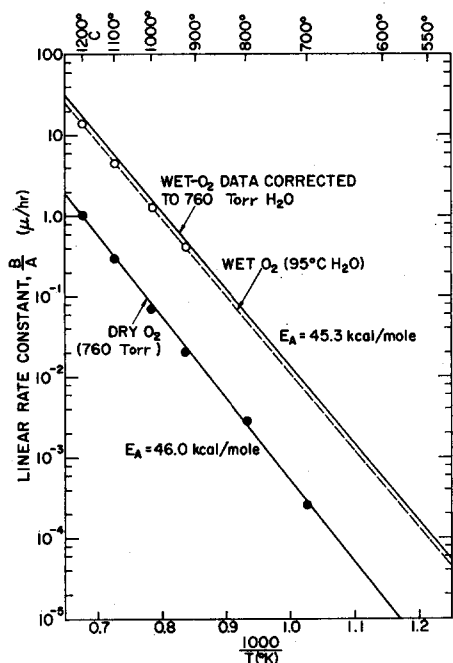
FIG. 12. General relationship for thermal oxidation of silicon. The solid line represents the general relationship, the dotted lines its two limiting forms. Experimental data were reduced using values of A and B determined from Figs. 8, 9, and 11. The values of τ correspond to $x_i=0$ and 200 Å for wet and dry oxygen, respectively.

characteristic time of the oxidation process,

$$\frac{A^2}{4B} = \frac{D_{eff}N_1}{2C^*(1/k+1/h)^2},$$

or, alternatively, that the oxide thickness should be smaller (or larger) than the characteristic distance of the oxidation process,

$$\frac{A}{2} = \frac{D_{eff}}{1/k+1/h}.$$

It should be noted that the general relationship, together with the rate constants from Figs. 9 and 11, corrected to the proper partial pressure according to Fig. 8, enables the construction of the correct oxidation-rate equation for any set of experimental conditions with confidence.

It is worthwhile to point out certain interesting aspects implicit in the results of this work. While the diffusivity of water in fused silica is lower than the diffusivity of oxygen (Fig. 10), the parabolic rate constant B is considerably larger for oxidation in wet oxygen than in dry (Fig. 9). This seeming paradox is immediately resolved when it is recalled that the flux of oxidant, and therefore the rate constant B is proportional to the equilibrium concentration C^*. This concentration is three orders of magnitude larger for water than for oxygen, thus accounting for the higher oxidation rate.

The existence of a rapid initial-oxidation stage with dry oxygen as well as the absence of such a phase with wet-oxygen oxidation are of interest. If the transported species is ionic, as has been shown to be the case for dry-oxygen oxidation by Jorgensen,[8] such a phase is

FIG. 11. The effect of temperature on the linear rate constant B/A.

to be expected[16] until such time that the oxide thickness becomes large in comparison to the extent of the space-charge region within the oxide. This latter quantity is of the order of the extrinsic Debye length of the oxide,[16]

$$L_{D,0} = [(kT/q)(K_0\epsilon_0/2qC^*)]^{\frac{1}{2}}.$$

Using the value of $C^* = 5 \times 10^{16}$ cm^{-3} as determined in this work, and the dielectric constant $K_0 = 4$, the oxide–Debye length is estimated to be of the order of 150 Å for dry O_2 oxidation, at 1000°C. This indeed corresponds well to the oxide thickness beyond which the rapid initial-growth mechanism stops being effective. In contrast, the extrinsic Debye length for oxidation in wet O_2, at 1000°C, using $C^* = 3 \times 10^{19}$ cm^{-3}, is estimated to be only around 6 Å. Thus, even if an initial rapid oxidation phase existed in the case of wet O_2, it could not be observed using the present techniques.

It is worthwhile to emphasize again that the good agreement between the pressure dependence of the coefficient B with the linear dependence expected on the basis of the assumption of Henry's law implies the absence of any dissociation effects at the gas–oxide interface. This, in turn, would imply that, for oxidation in wet oxygen, the diffusing species is undissociated water while for oxidation in dry oxygen it is molecular oxygen. The latter finding is in agreement with a similar conclusion reached by Norton[21] from the pressure dependence of permeation rate of oxygen through fused silica. Jorgensen[8] showed through experiments relating

to the effect of electric fields on dry-oxygen oxidation that the diffusing species is negatively charged. These two observations, taken together, point to the conclusion that the diffusing species in the case of dry-oxygen oxidation is the superoxide ion O_2^-. (For the properties of this ion, see Pauling,[24] p. 351.)

The field created by the space charge of the negatively charged oxygen ions should be directed toward the gas-oxide interface. Recent studies[25] of the Na^+ ion distribution in thermally grown oxides show that most of the Na^+ ions are concentrated near the outer surface after oxidation, in agreement with the above conclusion.

ACKNOWLEDGMENTS

APPENDIX

A simple criterion regarding the validity of the steady-state condition can be derived on the basis of an order-of-magnitude consideration, as follows. If the concentration distribution shown in Fig. 3 were disturbed, the return to equilibrium would take a period of time of the order of

$$t_{\text{transient}} \approx \frac{\text{total amount of oxidant needed to return to the steady-state distribution}}{\text{flux of oxidant}}.$$

Approximating the numerator by the total amount of oxidant present within the oxide layer in excess of a uniform concentration, i.e., $\frac{1}{2}(C_0 - C_i)x_0$, and the denominator by the flux F_2 as given by Eq. (4), the relaxation time is found to be of the order of

$$t_{\text{transient}} \approx x_0^2/2D_{\text{eff}}$$

in agreement with the result obtained by Fromhold[26] through a more detailed treatment.

For simplicity, taking $x_0^2 = Bt$,

$$t_{\text{transient}}/t \approx C^*/N_1 < 10^{-3}$$

in the parabolic region of oxidation—certainly a negligible time period.

[25] See abstracts of "Recent News" papers describing work of E. Yon, A. B. Kuper, and W. H. Ko, and of H. G. Carlson, C. R. Fuller, and J. Osborne, in J. Electrochem. Soc. 112, 259C (1965).
[26] A. T. Fromhold, Jr. J. Phys. Chem. Solids 24, 1081 (1963).